



MIE301 Final Report

Cire Rellid Parallel Planar Delta Mechanism

Group 14

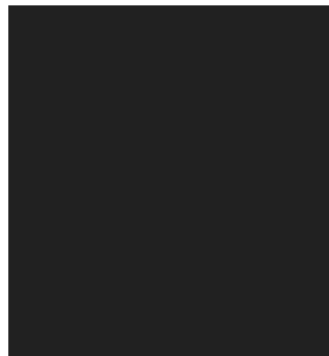
Dhruv Sharma

Dominik Adamiak

Mahin Choudhury

Percy Wu

Zakariya Khan



Submission Date: December 5, 2022

Contents

1	Introduction	1
2	Original Design Outline	2
3	Proposed 9-bar Mechanism in Response to Client Feedback	3
4	Analysis of Proposed 9-bar Mechanism	4
4.1	Analysis Goals and Methodology	4
4.2	Analysis	5
4.2.1	Finding Optimal Path for Mechanism Output	5
4.2.2	Developing Kinematically 6-bar Mechanism and Setting Link Length Constraints	5
4.2.3	Dynamic Force Analysis	6
4.2.4	Forward and Inverse Kinematic Equations	7
4.2.5	MATLAB Implementation for Large Scale Link Length Optimisation Testing	7
4.2.6	Optimal Solution Static Analysis	8
5	Results and Discussion for Optimal Solution of Redesigned 9-Bar PDM and FOC Summary	9
6	Conclusion	10
7	References	10

1. Introduction

In this report, Cire Rellid Linkages is proposing a redesign of its basic 5-bar planar (2D) delta mechanism in response to a request by client Eric Diller for a car manufacturing plant application. The client has requested a version of a 5-bar planar delta mechanism (PDM) which will lift small, lightweight plastic covers (mass = 150g) from a supply location to an assembly location on the vehicle roof rail, where a 10 N snapping force to the right will snap it in place. A typical delta robot is a three-dimensional mechanism that consists of three pairs of links which connect to a base on one end, and a moving platform on the other end with mobility = 6 [1]. The client has selected a planar delta design from our catalogue due to this type of robot being widely used in automated manufacturing to pick and place components with high speed in executing repeatable motions [1]. Since Cire Rellid's base 5-bar mechanism operates in the plane, it has two input linkages connected to two-bi directional servo motors, which can control the output motion with a mobility of two. After developing a set of functional engineering objectives and constraints in response to the client request in section 2, the base 5-bar design is deemed insufficient to meet the clients needs, since the original design can not constrain the end effector output angle in a way that allows all the objectives and constraints to be met. The proposed redesign, a 9-bar mechanism is proposed in section 3 and is fully analysed in section 4 to demonstrate the optimal configuration that best meets the client request.

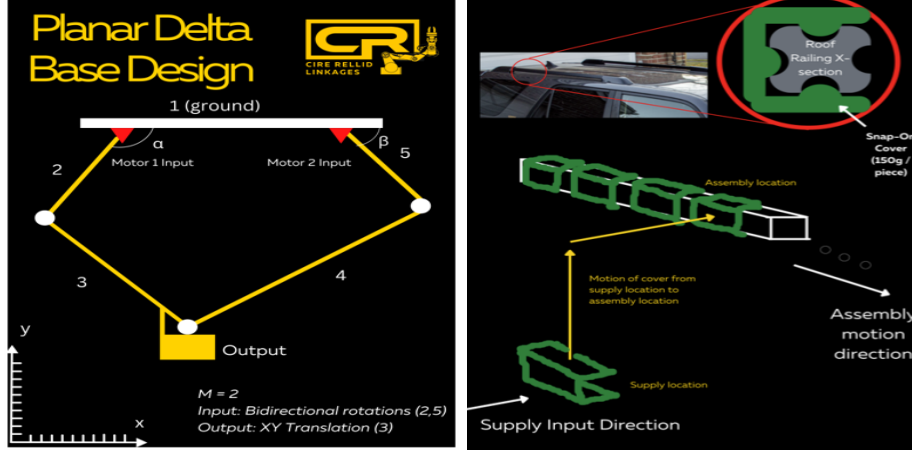


Figure 1. (a) Original 5-bar Mechanism Stick Diagram (b) Schematic of Client Assembly Process

2. Original Design Outline

The original design of the planar delta mechanism (PDM) was a 5-bar mechanism with a mobility of 2. It has two bi-directional servo motors at the kinematic turning pairs (2,3) and (4,5) that control the positional output attached to link 3 as in Figure 1a. Link 1 itself is the assembly line room roof, and the whole mechanism hangs from it, which is beneficial when compared to floor mounted manipulated if floor space is limited.

The most basic feature of the original 5-bar mechanism is the ability to control the output pair through a wide range of motion in the planar design space. Due to its low mass, high maneuverability, and low cost, it can be used in a host of assembly line operations to pick up and attach parts from one conveyor onto the vehicle frame (Figure 1b). Based on the client request, a series of functions, objectives and constraints (FOCs) can be developed, with regard to both industry standard operational cycle times, safety factors and assembly line dimensions and the client's needs for this application. These are detailed below in Table 1.

Table 1. Functions, objectives, and constraints of the project solution.

Functions	The PDM (planar delta mechanism) must move a small plastic car cover from a supply location to the car, and must snap it into its final assembly position.
Objectives	<p>O1 The output is parallel to the ground for the entire period of motion</p> <p>O2 Must be able to perform 20 cycles per minute^a</p> <p>O3 Must only use kinematic turning pairs</p> <p>O4* Design must minimize maximum motor torque required</p>
Constraints	<p>C1 Must be able to move 150g in mass with a safety factor of 1.5 [2]</p> <p>C2 The final output position must be parallel to the ground</p> <p>C3 Must deliver a 10N snapping force to the right at the final output position</p> <p>C4 Must move components from a feedtrack 150 cm upwards and 40 cm rightwards^b</p>

^aThe estimate for the amount of cars in a production line is 100 cars per hour [3]. Let each car need about 8 pieces of railing cover. This means 800 pieces per hour or 13.3 pieces per minute. Given a margin of safety of around 50%, this gives a target of 20 pieces per minute.

^bAverage height of a car is 150 cm [4] and the feedtrack is 40 cm away from the side of the car

In regards to the FOCs, it is apparent that a redesign must be made as this 5-bar design cannot meet certain objectives, namely **O1**. In the original design, the output must be fixed to either link

3 or link 4, both of which rotate, meaning that the output's angle cannot be controlled precisely. While it is possible to have the output parallel to the ground at the end of the movement path to meet constraint **C2**, this would mean that the starting angle of the part would be dependent on link lengths and the input/output positions. In this case, any form of optimisation which has link lengths and input/output positions as the independent variables (such as that of **O4***) will not be possible to perform (as a result of being constrained in a configuration that meets **C2**), and any client flexibility with path or input/output positions would not be possible. The objective **O4*** was initially an objective to minimise the motor energy required per cycle from both input motors. However, since the power consumption of medium scale servo motors is on the order of 1 kW, this is negligible when compared to the power demands of the client's automotive assembly line. Thus, it was determined that a more efficient objective would be to minimise the maximum torque the input motors experience during one cycle. This will allow a greater flexibility in choosing a smaller scaled motor, as well as improve the motor lifespan by reducing the fatigue wear. Lastly, constraint **C1** has been removed from the list of FOCs presented in the proposal report. Considering the small mass of the output ($m = 150\text{g}$), it is very unlikely that it will cause any kind of yielding or failure in 2cm diameter Al-T6061 tubes used here (the selection is discussed in section 4.1), which in this configuration has a radial yield force of 17 kN and axial yield force of 86 kN. The next section of this report explains the proposed design changes and how it meets the FOCs.

3. Proposed 9-bar Mechanism in Response to Client Feedback

As the original design is incapable of controlling the angular position of the output, it cannot mount the plastic covers correctly for a general combination of link lengths. A new proposed solution was found which addresses this issue. Our final proposed solution (see Figure 2) achieves an output parallel to the base link through the addition of two parallelogram linkages. The first parallelogram (green) consists of links 1a, 8, 9, and two points on 7, with opposing links equal in length. This parallelogram keeps the green link on 7 always vertical to the ground since 1a is fixed. The second parallelogram (blue) consists of links 5, 6, and two points each on 4 and 7 as shown. As long as the blue links on 4 and 7 are of the same length, they will be kept parallel to each other. The end result of this is that $\theta_4 = \theta_7 = 0$ for any combination of input angles. This means that the gripper attached to link 4 will never rotate - if the gripper starts parallel to the ground, it will always be parallel to the ground. Two other alternative proposals were also considered. One replaced a link with a sliding pair to control the output angle while the other used a motor on the output to directly control this angle. However, both alternatives require a third controlled and powered input which significantly increases complexity, production cost, and inertia (which would lead to slower cycle times). This final proposed solution was chosen above the other two alternatives as it does not require a third input while keeping the mass of the moving components relatively lightweight. This solution meets the FOCs as the rotational position of the output is parallel to the ground throughout its full range of motion.

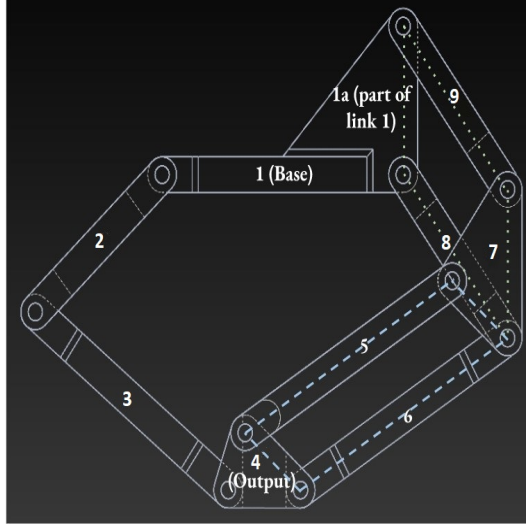


Figure 2. Final proposed 9-bar planar delta mechanism

4. Analysis of Proposed 9-bar Mechanism

4.1. Analysis Goals and Methodology

For our analysis, the primary goal is to minimise the maximum torque applied to the input motors (**O4***) during the assembly process at a minimum cycle time of 20 CPM (cycles per minute) (**O2**) using the 9-bar PDM, while meeting constraints **C1-C4**. The primary variables that will be optimised are the motion path of the output linkage from the supply to assembly positions, the rotational motor inputs, and the lengths of links 1-9 (subject to several geometric-design and simplification constraints for the optimisation to be possible, as will be discussed). Since a major objective **O1** is automatically satisfied by the design of the 9-bar (which was motivated from the original 5-bar to allow **C2** to be met for any possible path or link combination), the main analysis comparisons will be twofold. Firstly, we will trivially show that for some ideal combination of link lengths we determine for the 9-bar, a similar combination of links for the 5-bar does not satisfy **C2**. Secondly, and more relevant to this report, it will be demonstrated that within all possible designs of the 9-bar mechanism meeting the constraints, the proposed solution is optimal with regards to **O4*** while also meeting **O2**. For the optimal solution, the max motor torques of both motors will be shown over half a cycle to fully describe the mechanism operation alongside several sub optimal solutions, and the energy required by the motor will also be calculated by integrating the moment equation over θ of the inputs. Sources of error and approximation, limitations and future steps are also discussed in the conclusion.

The full algorithm for the 9-bar optimisation can be seen in Figure 3. In conducting the analysis, several assumptions were made. Firstly, due to the high acceleration of the PDM, inertial forces are non-negligible. Thus, a dynamic analysis must be conducted. However, due to the relatively small masses of the links, the gravity forces will not be included. The links themselves were taken as Al-T6061 (density, $\rho = 2730 \frac{kg}{m^3}$), with diameter = 2cm. Aluminum was specifically chosen because of its relatively high specific strength (the ratio of yield strength to density) compared to other metals [6]. Considering objectives **O2** and **O4***, the lightest material is the ideal choice to minimize the maximum motor torque. The links of certain high-end delta robots are made of carbon fiber reinforced polymers (CFRP) to minimize weight; however CFRP is significantly more costly than aluminum [7]. In lower-cost delta robots, such as the one offered to the client,

aluminum is more commonly used [8]. If we assume the links are either slender cylindrical rods or thin triangles, we can write the necessary moment of inertia formulations ($\frac{mr^2}{12}$ for cylinder, not required for triangle links as they are not rotating) that will aid us in conducting a dynamic force analysis. This approximation also means (assuming constant density) that mass of the links is directly proportional to length (or triangle link side length), which is also required for the force analysis. Lastly, the end effector output gripping mechanism was not modelled, as it is not relevant to the scope of kinematic motion analysis for the mechanism, and is instead left as an exercise to the eager reader.

4.2. Analysis

4.2.1. Finding Optimal Path for Mechanism Output

In our analysis, it was determined that the most optimal path of motion would be a straight line based on a few assumptions. First we started with the requirement that the output must stop before applying the necessary force to snap the part in place, as impulsive forces (if the part was not brought to a complete stop) are unpredictable and can damage the part. It was then assumed that the mechanism has linearity - that the motor torque is directly proportional to the acceleration. The fastest way that an object can move between two points is if the maximum acceleration is applied for half the duration, and the maximum deceleration is applied for the other half. By introducing the cycle time requirement of 3 seconds and the total displacement of 40 cm horizontally and 150 cm vertically, the constant acceleration kinematics equations can be used to solve for the required acceleration to meet these two requirements, in addition to the previous requirements of the initial and final velocities being zero. Solving the equations for both the horizontal and vertical equations separately to find acceleration and then integrating twice to obtain horizontal and vertical positions as a function of time, the time-parameterized plot of $(x(t), y(t))$ of the output was found to be a straight line.

4.2.2. Developing Kinematically 6-bar Mechanism and Setting Link Length Constraints

As seen in Figure 3, the 9-bar mechanism constrains the output angle to 0 during mobility 2 (x,y) motion via the supporting links 5, 2 and 4. We can remove these, and introduce an artificial mathematical constraint that $\theta_{output} = 0$ for all input angles.

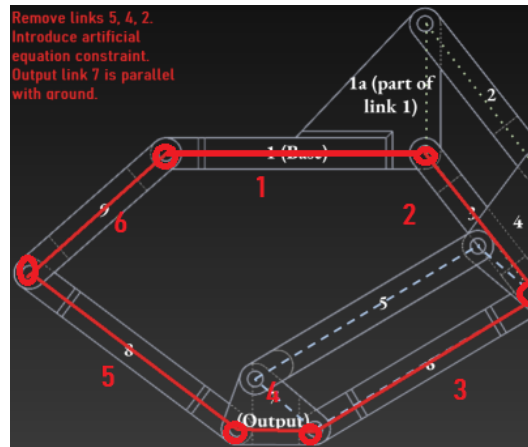


Figure 3. Kinematically equivalent 6-bar mechanism with artificial output constraint. Note that links are renumbered for purpose of vector loop analysis

In the analysis, a key symmetrical constraint of $r_6 = r_2$ and $r_5 = r_3$ was made. This was for two main reasons: computation time and initial output position calculation complexity. As will be shown in section D, in order to find the optimal set of links, the code must iterate through a range of link lengths for each link with nested for loops (one loop to iterate the length of each link). If there are n increments to check for each link length and it takes time t to calculate the properties of a set of link lengths, then the computation time is proportional to $(tn)^6$ when there are six unknown link lengths. By adding this constraint, this lowers the power from 6 to 4. This is necessary, as even with 4 unknowns the computation time with 10 logical CPU cores was over 7100 seconds for only n=10 length increments for each link, *after* a code speed optimization of over 200x.

In order to calculate the positions to get accelerations and moments, the initial position of the output (defined as the lowest point that the mechanism can extend to) must be first determined in the inverse kinematics code. In the case of this symmetrical constraint, it is easy to find as it is simply a trapezoid. However, should there be asymmetry, the cases of all the different shapes for different combinations of relative link lengths must be considered, with equations written separately for each case. This further increases both calculation complexity and computation time.

4.2.3. Dynamic Force Analysis

In an arbitrary configuration, the equations for sum for forces in the x,y and the sum of moments can be written for each link in the 9-bar mechanism, as seen in 5 below. Using the equations of moment of inertia for slender rods, we can eliminate forces by taking moments about ground pivots in the 3 links connected to ground. Other eliminations can be made by using the concept of 2-force links, noting that the angular velocities of the triangle links = 0, and that the overall accelerations of each set of parallel links is the same. In the end, a system of 24 equations in 24 unknowns (equation A) is developed to describe the forces and moments present in all parts of the mechanism for some output position and acceleration. The following equations show examples of the three categories of links we encounter (refer to Figure 4(a) for the free-body diagram):

Link 2 (attached to ground - Link 8 and 9 are similar):

$$\vec{F}_{12} + \vec{F}_{32} = m_2 \vec{a}_2$$

$$M_{alpha} - \vec{r}_2 \times \vec{F}_{32} = (I_G + md^2)\alpha_2$$

Link 3 (attached to another link - Link 5 and 6 are similar):

$$\vec{F}_{43} - \vec{F}_{32} = m_3 \vec{a}_3$$

$$0.5\vec{r}_3 \times -\vec{F}_{32} - 0.5\vec{r}_3 \times \vec{F}_{43} = I_G \alpha_3$$

Link 4 (triangle - Link 7 is similar):

$$\vec{F}_{43} + \vec{F}_{54} + \vec{F}_{64} = m_4 \vec{a}_4$$

$$\frac{F_{43y}L_4}{2} - L_4 F_{43x} \frac{\sqrt{3}}{6} + L_4 F_{64x} \frac{\sqrt{3}}{6} + \frac{F_{64y}L_4}{2} - L_4 F_{54x} \frac{\sqrt{3}}{3} = 0$$

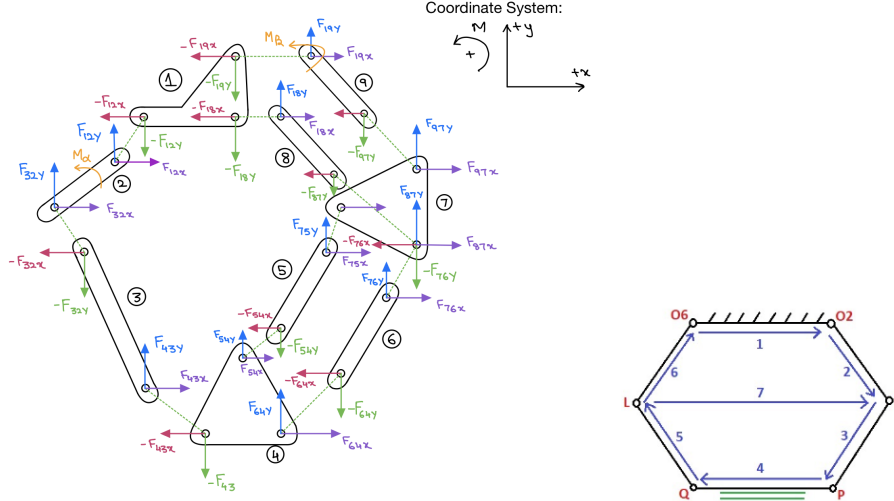


Figure 4. (a) Dynamic Force Analysis on 9-bar PDM. (b) Vector Loop for 6 .

4.2.4. Forward and Inverse Kinematic Equations

The goal of the analytical inverse equations is to fully define the position of every link in the mechanism depending on the output angle. Since the link lengths are known in addition to the angular position of links 1 and 6 for all time, the angles of links 2,3,5, and 6 must be calculated. Based on Figure 4(b), the equation for point \vec{P} is (note that point O_6 was defined as $(0,0)$):

$$\vec{P} = \vec{R}_1 + \vec{R}_2 + \vec{R}_3 \rightarrow [P_x, P_y] = [r_1 + r_2 \cos \theta_2 + r_3 \cos \theta_3, r_2 \sin \theta_2 + r_3 \sin \theta_3] \quad (1)$$

To find θ_2 , we must cancel θ_3 in equation 1. Moving θ_3 to the left hand side and P terms to the right gives

$$-r_3 \cos \theta_3 = r_1 + r_2 \cos \theta_2 - P_x \quad (2)$$

$$-r_3 \sin \theta_3 = r_2 \sin \theta_2 - P_y \quad (3)$$

Squaring both sides and applying $\sin^2 \theta_3 + \cos^2 \theta_3 = 1$,

$$r_3^2 = (r_1 + r_2 \cos \theta_2 - P_x)^2 + (r_2 \sin \theta_2 - P_y)^2 \quad (4)$$

By passing equation 4 into Wolfram Mathematica (<https://www.wolframcloud.com/obj/e7505280-7ef9-494f-bce4-23467c3564c3>) and solving for θ_2 (selecting the two correct solutions by graphical trial and error in MATLAB), the correct solution was found. The solution for θ_3 was found similarly by moving θ_2 terms to the left hand side such that they reduce to r_2^2 when squared. θ_6 and θ_5 were calculated in the same way, through the vector equation $\vec{Q} = -\vec{R}_6 - \vec{R}_5$.

4.2.5. MATLAB Implementation for Large Scale Link Length Optimisation Testing

Knowing the forward and inverse kinematics, as well as knowing the dynamic formulation for the PDM, we now use a MATLAB code to determine the optimal linkage lengths for minimising maximum motor torque (**O4***) in the straight line path (section 4.2.1), subject to the necessary

link constraints developed in section 4.2.4. The full algorithm is shown in Figure 5 below, and it involves cycling through various combinations of links lengths, given some length resolution and time step resolution. In our analysis, the mechanism was simulated over 45 timesteps over one half cycle (since the other half is simply the reverse path), where for each timestep every combination of link sizes from roughly 0.1-4 m is tested for motor torques. In lieu of analytically determining limit positions and constructable link combinations (by ensuring the link lengths satisfy some union of forward/inverse kinematic equation domains), various exception statements in the code checking for imaginary outputs and division by 0 are used to eliminate impossible linkage length combinations. This is because an analytical solution would be in terms of the 4 unknown linkage lengths, and would result in very inefficient MATLAB run times. The full algorithm is shown below in Figure 5:

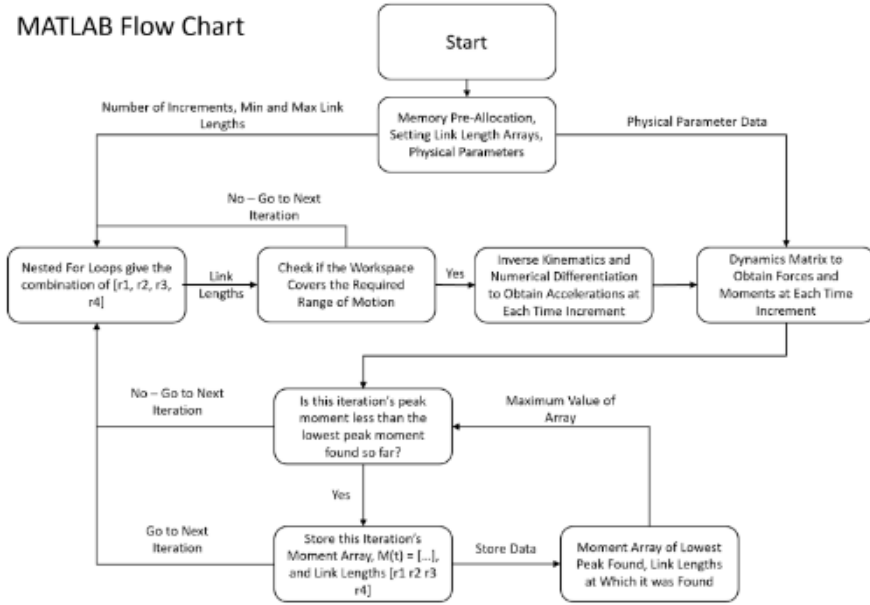


Figure 5. MATLAB code algorithm for solving for optimal linkage length combinations in 9-bar PDM

4.2.6. Optimal Solution Static Analysis

After obtaining the desired link lengths from the Dynamic Analysis on the simplified 6-bar mechanism, the mechanism was validated and motor torques were calculated for the output position of the mechanism by conducting a static analysis of the mechanism using the Free Body Diagram in Figure 4(a). Since the link lengths are now known, the MATLAB code was redefined to determine the output angles of the mechanism assuming zero inertial forces and acceleration of the links, weightless links, and the net Moments at all links to be zero.

The net horizontal force at the output link was equated to -10N (to the left) and the horizontal components of the forces were determined using the system of equations to get the following values:

$$F_{output} = -F_{43x} + F_{54x} + F_{64x}$$

$$\text{where } F_{43x} = -10.0248N, F_{54x} = -0.1122N, F_{64x} = 0.0874N$$

As a result, we get

$$F_{output} = 10N$$

Now, for the motor torques, it was determined that the left motor has an output torque of 4.066 Nm and the right motor has an output torque of 0.934 Nm (both are positive in the anticlockwise direction)

5. Results and Discussion for Optimal Solution of Redesigned 9-Bar PDM and FOC Summary

Through preforming the dynamic optimisation, the optimal 9-bar linkage dimensions are 0.4, 0.8, 1.2, 0.4, 1.2, 0.8, 0.4, 0.8, 0.8 m for link lengths r_1 through r_9 . With these values, we achieve the smallest possible maximum torque of 12.3 Nm (left motor) at $\theta = 85.9$ and 28.8 Nm (right motor) at $\theta = -23.2$ degrees. The torques required for the 10 N pushing force are below this magnitude, satisfying **C3**. Over half a cycle, the most-optimal 9-bar solution left and right input motor torque magnitudes are plotted in Figure 6a. Similarly, the maximum right motor torques of several other sub-optimal combinations of link lengths are plotted alongside the optimal in Figure 6b, which clearly demonstrates that the solution found has the smallest torque peak, and has the smoothest profile (which will help with motor wear), objective **O4***.

In addition, a similar link length combination 5-bar solution output angle is plotted vs. time over half a cycle in Figure 6e, showing how the original mechanism will not be able to satisfy **O1** and **C2**, **C3** In addition, the motor angle and angular velocities are plotted versus time are plotted in Figures 6c, 6d The left and right motor works are calculated as 8J and 53.8 J per half cycle, which is almost negligible, as expected. Evaluating our remaining objectives, we find that the cycle time of our mechanism is 3 s, which leads to a cycle time of 20 cycles/min, which meets the requirement **O2**. The design simplicity in only using kinematic pairs (**O3**) is also evident in the design of the 9-bar PDM. Finally, constraint **C4** is met by a simple plot of the output x vs. y position.

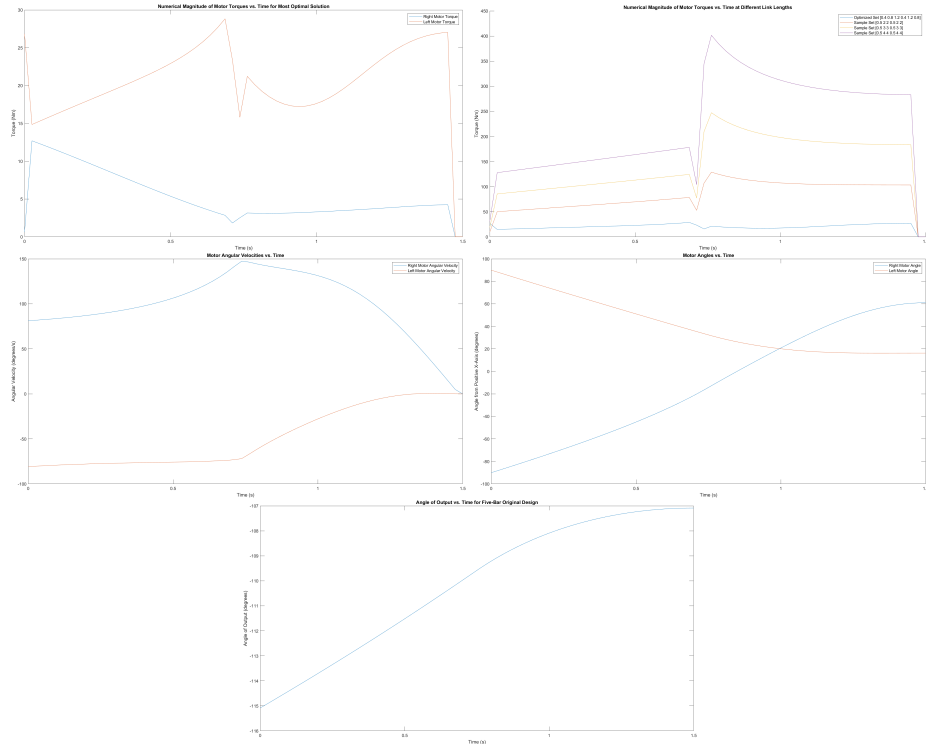


Figure 6. (a) Motor Torques over half-cycle for Optimal Solution (b) Suboptimal 9-bar solutions (c) Optimal motor velocities and (d) angles over half-cycle (e) 5-bar output angle over half cycle

6. Conclusion

Using the methodology outlined in section 4, and based on the FOCs developed in section 2, the optimal path (straight line over half a cycle) and link length combination of (.....) fully determined for the design of the client's optimal custom 9-bar PDM. The specific results of the maximum-torque minimising design are outlined in section 5, and it will allow the client to most efficiently supplement the operation of his automobile factory. In this analysis, there are several important limitations that must be noted, in addition for several potential avenues for future work. These include:

- A small timestep resolution of 45, and length resolution of 10 which limited the accuracy of the numerical plotting of analytical solutions due to CPU limitations
- The symmetry linkage length constraint for the forward and inverse kinematic equations which potentially limits more optimised solutions from appearing as outputs in the MATLAB script
- Assuming gravity force is negligible to simplify the kinematic and dynamic equations introduces a slight error in the absolute magnitude of the maximum torque recorded. However, since this is a linear system the principle of superposition tells us that it should not influence what is the most optimal link length combination.

In extending this work, focus should be placed on developing a different approach in solving the kinematic equations using more advanced methods than simply a vector loop approach, which is likely to result in a more elegant form of optimisation. In addition, the code used cycle through all the possible permutations of linkage lengths is very unoptimised, having a run time of 7141 seconds (2 hours) during the final dynamic analysis. Other future areas of work include the design of the end effector (output) gripper, and a more thorough investigation of the workspace limits. Heavier load applications will also require the inclusion of a simple stress analysis, but the overall flexibility of this analysis means it can be modified for many different client demands.

7. References

- [1] Rey, L., Clavel, R. (1999). The Delta Parallel Robot. In: Boër, C.R., Molinari-Tosatti, L., Smith, K.S. (eds) Parallel Kinematic Machines. Advanced Manufacturing. Springer, London. https://doi.org/10.1007/978-1-4471-0885-6_29.
- [2] R. Beardmore, "Basic Notes on Factor of Safety," RoyMech. [Online]. Available: https://roymech.org/Useful_Tables/ARM/Safety_Factors.html [Accessed: 03-Nov-2022]
- [3] L. Kilchermann, "What happens on a car assembly line?," About Mechanics, 07-Oct-2022. [Online]. Available: <https://www.aboutmechanics.com/what-happens-on-a-car-assembly-line.htm>. [Accessed: 03-Nov-2022].
- [4] "2.5 average car height, width and weight, 1980-2018," Mobiliteit in Cijfers Auto 2019. [Online]. Available: <https://bovagrai.info/auto/2019/en/2-registrations/2-5-average-car-height-width-and-weight/>. [Accessed: 03-Nov-2022].
- [5] Teknic, "ClearPath Integrated Servo Motors," teknic.com. <https://teknic.com/products/clearpath-brushless-dc-servo-motor/?gclid=Cj0KCQiAyracBhDoARIsACGFcS7Us4h0UrDnueoBenGayiC8jBLMVh2PVMlaAsDoEALwwcB> (accessed Dec. 1, 2022).
- [6] "Aluminum 6061-T6; 6061-T651," matweb.com. <https://www.matweb.com/search/DataSheet.aspx?MatGUID=b8d536e0b9b54bd7b69e4124d8f1d20a&ckck=1> (accessed Dec. 1, 2022).
- [7] Ensinger Plastics, "Composite robotic arm," ensingerplastics.com. <https://www.ensingerplastics.com/en-us/engineering/robotic-arm-packaging> (accessed Dec. 2, 2022).
- [8] P. Heney, "igus Delta Robot a Low-Cost Option for Assembly Tasks." therobotreport.com. <https://www.therobotreport.com/igus-delta-robot-cost-effective-assembly/> (accessed Dec. 2, 2022).